 FDMP, vol.3, no.3, pp.247-254, 2007

Modeling a Discontinuous CVD Coating Process: I. Model Development and Validation

Joseph G. Lawrence and Arunan Nadarajah[1]

Abstract: A simplified 2D pseudo steady state model was developed for an atmospheric chemical vapor deposition (CVD) process on glass. This is used to study the feasibility of converting a continuous coating process to one with discrete glass plates with a gap between them. A preliminary estimate employing mass transfer correlations suggested that there would be significant concentration variations due to the gap between the plates. More detailed studies were done by solving the model numerically employing a finite difference scheme with a vorticity-stream function formulation, and employing the commercial computational fluid dynamics program FIDAP which employs a finite element scheme. The equations for the velocity profile in the model were solved with both methods and node by node comparisons were carried out. The results showed close agreement between both approaches which indicated the applicability of the FIDAP program to this problem. The results also indicated the validity of the pseudo steady state model developed here. In a subsequent study a more detailed model was employed with FIDAP to examine the effect of the gap between the plates on the CVD coating process [Lawrence, J.G.; Dismukes, J.P.; Nadarajah, A. (2007): FDMP: Fluid Dynamics & Materials Processing, vol.3,no.3,pp.255-264.].

Keyword: CVD, Glass, Numerical Simulations, Coatings.

1 Introduction

Chemical vapor deposition (CVD) on glass is an essential coating process for many applications, including automotive windshields, doors of large consumer appliances such as conventional and microwave ovens, and windows used in buildings. CVD glass coating was initially employed during the 1970's to produce reflective mirror products [Callies, Albach, Conour and Herrington (1987)]. Since then various coater designs and modifications have been developed according to needs. A continuous online atmospheric CVD coater was jointly developed by Gordon (1997) and McCurdy (1999) and was used for silicon deposition from gaseous silane on continuous sheets of glass.

This work examines the feasibility of transforming this continuous coating process to a discrete one. In the discrete process, glass arrives at the coater as individual plates with gaps between them. The modified coating process is illustrated in Fig. 1. The central concern in this modification is its influence on the uniformity of the coating. The presence of the gap between the plates will result in non-uniform gas flows and may cause edge effects on the coatings.

While the effect of the discontinuity can be investigated experimentally, this is an expensive and time consuming proposition. Mathematical modeling offers a much better alternative and has the added advantage of providing a fundamental understanding of the gas flow and mass transfer processes for this application [Meyappan (1995)]. The commercial availability of computational fluid dynamics (CFD) software packages that can simulate a wide variety of industrial processes further facilitates such studies. However, before they can be utilized for reliably predicting process behavior, the commercial software packages must be validated for that particular system.

This problem was analyzed in three stages. First,

[1] Department of Chemical and Environmental Engineering, University of Toledo, Toledo, Ohio 43606, USA. Corresponding author: nadarajah@utoledo.edu

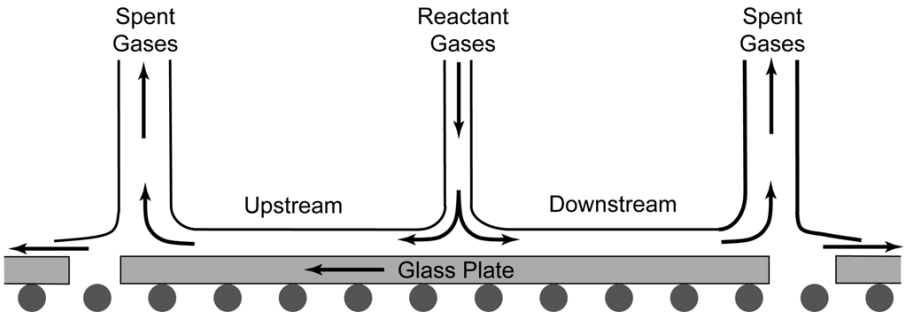

Figure 1: Schematic of CVD coater with discrete glass plates. The plates move on rollers through the stationary coater. The gaps between the plates are visible.

a simplified analysis employing mass transfer correlations was carried out to estimate the effect of discrete plates on the uniformity of the coating. The purpose of this analysis was to provide a rapid estimate of the magnitude of this effect in order to decide if further analysis is necessary. Second, a simplified analytical model was developed, along with a numerical scheme for solving it. The model was also solved with a commercial CFD program and the results from the two approaches were compared. This allowed us to test the validity of the commercial program to this problem. The validation allowed the third and final stage of this analysis to be carried out. This involved the development of a more comprehensive model and its solution solely with the CFD program and this will be reported in a subsequent publication [Lawrence, Dismukes and Nadarajah (2006)]. This study will focus on the first two stages.

2 Development of the Model

The 2D mathematical model was developed from the existing coater design [Zhu (2000)] by using simplified assumptions. Of particular interest in this model was the inclusion of the gap between the plates and their effect on the deposition process. Neglecting the short stages when the gap is directly below the reactant gas inlet and the spent gas outlet, the model will focus on the process when the gap is between them. Even in this region, unlike in the continuous process, the presence of the gap makes this a moving boundary problem. The complexity of solving such a problem may obscure the result that is important here: effect of the gap on the deposition rate. As a result, a pseudo-steady state model was employed which freezes the location of the gap.

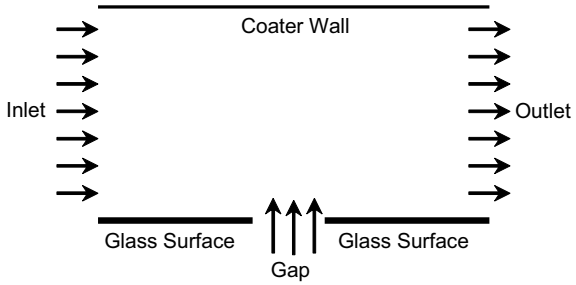

Figure 2: Section of the reactor used for numerical analysis.

The basis for the pseudo steady state model is the very high gas flow rates compared with the slow rate at which the plates move through the coater. Any local flow effects due to the plate motion are, therefore, negligible. This also means that location of the gap relative to the inlet (i.e. upstream or downstream), will also have a negligible effect. The only effect of this motion is on the location of the gap and how it affects the flow field at that instant. Thus, a reasonable approach is to model this by a pseudo-steady state model with the gap in a fixed position and the gases flowing steadily. By carrying out different steady state simulations with the gap at different positions, it will be possible to examine the effect of gap motion on the coating process. The 2D model geometry is shown in Fig. 2. The inlet

gases are assumed to be well mixed. Any reactions in the gas phase are neglected, and the only reactions considered are those with glass surface due to the deposition.

The inlet concentration of the coating gases was assumed to be 6% by weight [McCurdy (1999)] with a volumetric flow rate of 4.78 slpm. For these conditions the Reynolds number (Re) was found to be between 7 and 25, which means the flow is laminar. When the Grashof number (Gr) was calculated, it was found that $(\mathrm{Gr}/\mathrm{Re}^2) \sim 0.2 < 1$. This means natural convection is much smaller than forced convection and its effects can be neglected [Curtis and Dismukes (1972)]. The dominance of forced convection in this problem also suggests that temperature and concentration variations will be moderated in this process.

Even with the moderation of variations in temperature and concentration, there can still be significant variations in physical properties, such as density, viscosity, conductivity, and specific heat. However, if natural convection is excluded, none of these variations will fundamentally affect the transport process in the reactor. Most importantly, these variations have little or no effect on the phenomena of primary interest in these simulations, namely the uniformity of the coatings. As a result the physical properties may be assumed to be constant for these simulations. However, given its direct relation to the coating process, the temperature dependence of the deposition rate constant was retained.

The chemical reactions in most metal oxide CVD processes are extremely complex. The focus of this study is on the uniformity of the coating process which is more a function of the mass transport processes in the reactor than the chemical reactions. As a result any chemical reactions in the gas phase will be neglected and only the silane decomposition to coat the glass will be considered as a simple first order reaction boundary condition. With these assumptions, the set of equations for this study consists of the 2D conservation equations of mass, momentum, energy, and species mass balance for the velocity $\boldsymbol{v}$, pressure P, temperature T and species concentration C as given below [Slattery (1999)]:

$$\nabla \cdot \boldsymbol{v} = 0, \tag{1}$$

$$\rho \boldsymbol{v} \cdot \nabla \boldsymbol{v} = -\nabla P + \mu \nabla^2 \boldsymbol{v}, \tag{2}$$

$$\boldsymbol{v} \cdot \nabla T = \alpha \nabla^2 T, \tag{3}$$

$$\boldsymbol{v} \cdot \nabla C = D \nabla^2 C. \tag{4}$$

Here ρ is the density, μ the viscosity, α the thermal diffusivity and D the species diffusivity.

The boundary conditions for velocity are given below.

At the inlet: $v_y = 0$ and $v_x = Q/A_i$, where Q is the inlet volumetric flow rate and A_i the inlet cross-sectional area.

At the top wall: $v_y = 0$ and $v_x = 0$.

At the bottom glass plates: $v_y = 0$ and $v_x = -V$, where V is the constant small velocity of the glass plates through the coater.

At the outlet: $\int \boldsymbol{v} \cdot \mathbf{n} dA = bias \cdot Q$.

At the gap: $-\int \boldsymbol{v} \cdot \mathbf{n} dA = (bias - 1)Q$, where the bias is the ratio of coating gas flow rate at the outlet vent to the inlet gas flow rate. The mass flow rates at the outlets depend on the specified bias.

The temperature boundary conditions are given below. The temperature at the walls and the gas inlet are considered to be equal since the walls of the reactor are preheated to the temperature of the gases before they enter the reaction chamber. The temperature of the entering gas at the gap could be lower as it passes through unheated sections of the coater, but it will be heated when it passes by the superheated rollers and glass plates. As a result the temperature of the gas entering through the gap is assumed to have the same temperature as the inlet gas.

At the inlet, top wall and gap: $T = T_1$

At the bottom glass plates: $T = T_{ref}$

The boundary conditions for species concentration are specified at the glass surface as a simple first order reaction. The temperature dependence of chemical reaction is in the form of the Arrhenius equation. The heat generated by chemical reaction on the glass surface was estimated to be 1.1 kJ/s, while the heat transfer rate from the gases to

the glass surface was 45 kJ/s. Comparing the two values, the heat generated due to chemical reaction was neglected.

At the inlet: $C = C_{ref}$. At the top wall: $\partial C/\partial y = 0$

At the gap: $C = 0$

At the bottom glass plates: $D\partial C/\partial y = k_0 \exp(-E/RT)\cdot C$,

where k_0 is the pre-exponent, E is the activation energy of the deposition reaction and R the universal gas constant.

3 Estimates from Correlations

Before attempting to solve the domain equations numerically, an initial estimate of the concentration along the length of the coater was obtained by using correlations. The concentration variation from the leading edge of a discrete glass plate can be readily estimated in this manner. From the fluid properties in Table 1 [Dean (1992), Perry and Green (1984)], the dimensionless numbers were calculated. The value for mass transfer Prandtl number (Pr) was 0.1 which indicates that the process is in the laminar low Prandtl number region.

Table 1: Properties of inlet gases at 600K. Since nitrogen is the principle component of the inlet gases its properties are employed in the simulations.

Physical Property	**Value**
Viscosity μ	2.96×10^{-5} Ns/m^2
Thermal conductivity κ	0.044 W/mK
Heat capacity C_p	1 kJ/kg·K
Density ρ	0.60 kg/m^3
Diffusivity D	0.849×10^{-4} m^2/s
Coeff. of thermal expansion β	1.43×10^{-3}
Reaction rate constant k at 573K (Silane decomposition)	5 s^{-1}
Activation energy E (Silane decomposition)	1.7 eV

The correlation for local mass transfer coefficient for low Pr laminar flow over a flat plate is given by $Nu_x = 0.564 Re_x^{0.5} Pr^{0.5}$ [Welty, Wicks and Wilson (1984)]. From the value of Nu_x, the local mass transfer coefficient k_D can be calculated from $k_D = Nu_x D/x$, where x is the distance downstream from the leading edge. From the value of k_D, the mass transfer flux J_y is calculated using the equation $J_y = k_D(C_\infty - C_s)$. The surface concentration C_s is taken to be zero at the surface as the concentration of the gas drops to zero on the glass surface as a result of chemical reaction. C_∞ is calculated as the bulk concentration using 6 mol% of silane gas. The deposition rate at the surface of the glass is obtained by dividing the mass transfer flux by molar density of the solid.

While this method of calculation may not provide accurate results for the local mass transfer rate, it can be useful in obtaining an initial estimate of the concentration at various points in the reactor. From the values of deposition rate it was observed that, there was a ∼35% decrease in deposition rate at a distance midway from the entrance of the reactor and ∼60% decrease near the outlet. These simple estimates suggest that there may be non-uniformity in coatings and edge effects may be significant. This warrants carrying out detailed numerical simulations of this process in order to study these effects.

4 Numerical Simulations

For numerical analysis, the domain equations and boundary conditions are conveniently expressed in dimensionless form. The non-dimensional representation can be achieved by properly choosing the characteristic quantities. The non-dimensional quantities are defined as:

$\boldsymbol{v}^* = \boldsymbol{v}/v_{ref}$, $L^* = \rho v_{ref} L/\mu$, $P^* = P/P_{ref}$, $P_{ref} = \rho v_{ref}^2$,

$T^* = \frac{T - T_{ref}}{T_1 - T_{ref}}$, $C^* = C/Cref$,

where v_{ref} is a reference velocity magnitude, T_{ref} the temperature of the glass plate, T_1 the inlet gas temperature and C_{ref} the inlet concentration. After replacing the dimensional quantities in the domain equations 1 to 4 by non-dimensional quantities, the following non-dimensional form of the

governing equations are obtained:

$$\nabla \cdot \boldsymbol{v}^* = 0, \tag{5}$$

$$\boldsymbol{v}^* \cdot \nabla \boldsymbol{v}^* = -\nabla P^* + \nabla^2 \boldsymbol{v}^*, \tag{6}$$

$$\mathrm{Pr}\,\boldsymbol{v}^* \cdot \nabla T^* = \nabla^2 T^*, \tag{7}$$

$$\mathrm{Sc}\,\boldsymbol{v}^* \cdot \nabla C^* = \nabla^2 C^*. \tag{8}$$

Here Sc is the Schmidt number given by $\mu/\rho D$.

After defining the domain equations and boundary conditions in dimensionless form, the problem was solved numerically with a finite difference code and the commercial CFD program FIDAP [FIDAP (1998)]. For this comparison study the solution was restricted to the velocity profile only. This should be sufficient to verify the applicability of the FIDAP program to this problem. For the finite-difference approach the velocity profile is obtained by solving the conservation equations of mass and momentum, employing the artificial compressibility method [Chorin (1997); Abdallah (1987)]. In this method, the conservation of mass equation is modified in such a way to include an artificial compressibility term that vanishes when the steady-state solution is reached. With the addition of this term to the conservation of mass equation, the resulting Navier-Stokes equations are a mixed set of hyperbolic-parabolic equations. These equations can be solved using a standard time-dependent approach.

A vorticity-stream function formulation was used to transform the velocity components in terms of the derived variables: stream function and vorticity. In this approach, the conservation of momentum equations in x and y directions can be combined to give the single vorticity transport equation shown below:

$$u\frac{\partial \zeta}{\partial x} + v\frac{\partial \zeta}{\partial y} = v\left(\frac{\partial^2 \zeta}{\partial x^2} + \frac{\partial^2 \zeta}{\partial y^2}\right). \tag{9}$$

The conservation of mass equation when modified using the vorticity ζ and stream function ψ, takes the form of the Poisson equation:

$$\frac{\partial^2 \psi}{\partial x^2} + \frac{\partial^2 \psi}{\partial y^2} = -\zeta \tag{10}$$

Equations 10 and 11 are discretized using central difference (implicit) method. In the vorticity-stream function formulation, the flow rate across, a line beginning and ending at two planes located at $y = y_1$ and y_2 is equal to the difference in the corresponding values of the stream functions $Q_{12} = \psi(y_2) - \psi(y_1)$.

The boundary conditions are changed appropriately in terms of vorticity and stream functions. The vorticity boundary conditions are specified for wall motion and the stream function boundary conditions are specified at the walls. The transformed boundary conditions are:

$\psi = 0$ at the glass surface,

$\psi = 1$ at the top wall,

$\partial\psi/\partial y = 0$ at the inlet and

$-\partial\psi/\partial x = 0$ at the gap.

These equations are solved using the methodology suggested by Pozrikidis (2001). An initial guess is made on the stream function distribution and associated vorticity. Equation 11 is solved for the stream function subject to boundary conditions. The value for the quantity in the parenthesis in equation 10 is computed and the boundary conditions for vorticity are derived using the stream function obtained earlier. The Poisson equation is solved for the vorticity and the computed value of vorticity is checked with the assumed value to be within specified tolerance. The calculations were repeated by replacing the later value with the former until the required convergence was reached. The no-penetration and no-slip boundary conditions are enforced in a sequential fashion, the no-penetration conditions are enforced in the process of solving the stream function, and the no-slip condition is enforced in the process of deriving boundary conditions for the vorticity.

The solution methodology described above was incorporated in a FORTRAN code, solved for stream function and vorticity and the results plotted using MATLAB. From the streams functions, the x and y components of velocity were calculated. Total number of iterations and value of the residual were specified to achieve a converged solution.

The domain equations and boundary conditions

mentioned above were also incorporated in the FIDAP code. The velocities at the gaps are not specified, and the gaps are specified as vents in the simulation command. At the vents the velocity profile is determined from the solution of rest of the flow domain. The velocity boundary conditions are set according to the mass balance across the reactor. Hence depending on the bias applied there may be inflow or outflow of gases at the vents.

In the case of FIDAP simulations, the set of partial differential equations that describe the system (the continuum problem) are reduced to a set of algebraic equations (discretized problem) using the Galerkin form of the method of weighted residuals. The method used for solution in this particular case is the Newton-Raphson method. The dimension, mesh and number of nodes were kept the same as in the finite-difference method. The results obtained with FIDAP modeling and from finite-difference code were compared point to point to check the validity of the commercial code for this problem.

5 Results and Discussion

Velocity vector and contour plots were obtained in both the simulations and are shown in Figs. 3, 4, 5 and 6. The dimension of the reactor used for comparison of codes was 15 cm in length and 5 cm in width with 5 cm gap between the glass plates. The maximum velocity in the flow field was taken as the reference velocity to obtain the dimensionless velocity. The inlet velocity in dimensionless form had a value of 0.75 with a bias of 1.5 at the outlet. The velocity vector and contour plots for the finite difference and FIDAP simulations were obtained with a bias of 1.5.

These figures clearly show that the flow fields are laminar and that the presence of the gap between the plates did not produce turbulent eddies. The effect of the bias on the flow field is also clearly shown in these figures with significant inflows through the gap. More significantly, it can be seen that the flow field is dominated by the gas flows at the inlets rather than the plate motion. This suggests the validity of the pseudo-steady state model developed for this problem. These simulations can be considered as snapshots of the process as the gap between the plates move along the bottom wall.

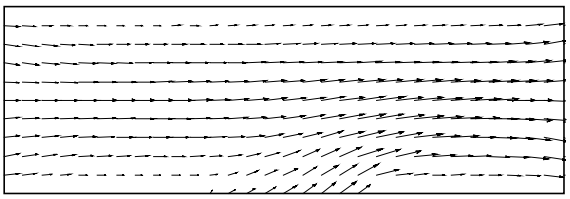

Figure 3: Velocity vector plot from FIDAP simulation for a bias of 1.5 and inlet velocity of 0.75.

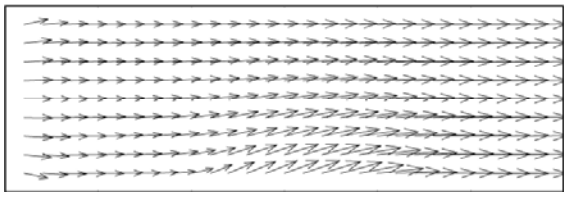

Figure 4: Velocity vector plot from finite-difference simulation for a bias of 1.5 and inlet velocity of 0.75.

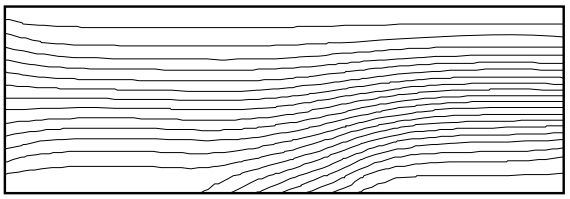

Figure 5: Stream function contour plot from FIDAP simulation for the case shown in Fig. 3.

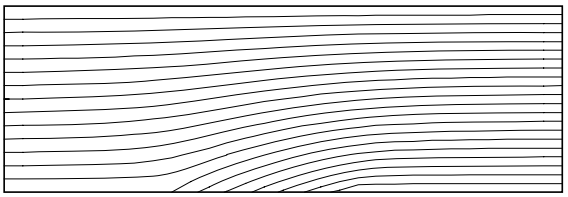

Figure 6: Stream function contour plot from finite-difference simulation for the case shown in Fig. 4.

Visual comparisons of these plots indicate that the results obtained from both the simulations are qualitatively similar. In case of finite-difference simulation, velocities were obtained by differentiating the stream function values at the nodes. The contour plots appear to be similar and this suggests that the two simulation results are the same. Although not shown here, simulations were carried out at other conditions and they produced similar results.

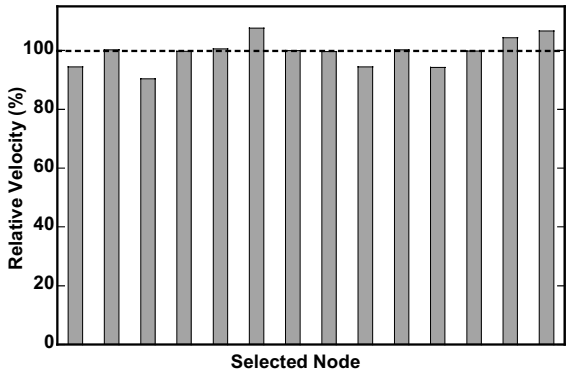

Figure 7: Comparison of results obtained from FIDAP and finite-difference simulations. The x component velocities from the FIDAP simulation are taken to be 100% at each node point and the corresponding values from the finite difference simulation are shown as bars.

In order to carry out a more careful comparison between the results from the two methods, node-by-node comparisons of the x component of velocities, obtained from the finite-difference and FIDAP simulations, were done. One such comparison is shown in Fig. 7. For this case the nodes were chosen randomly at different points in the solution domain. The comparison chart shown in Fig. 7 shows that variations were small. Other node-by-node comparisons produced similar or better results.

For the simplified geometry and reasonable assumptions made, the finite difference code and FIDAP code produced similar results. Given that finite difference methods have lower orders of accuracy than finite element methods, this close agreement between them strongly suggests that these are the correct solutions to the problem. This validates the applicability of FIDAP for this particular problem.

The advantage of employing FIDAP over the finite difference code is that in addition to the velocity profiles considered here, temperature and species concentration profiles can easily be obtained and more complex geometries and boundary conditions can be implemented. FIDAP was used for all subsequent simulations of the complex model and these results will be reported later.

6 Conclusions

An estimate based on mass transfer correlations suggested that for the problem of atmospheric CVD on discrete glass plates in a coating system, there could be significant variations in deposition rates across the plates. A simplified 2D model of the process that employs a pseudo steady state approach was developed to further analyze the problem. The results from numerical simulations suggested that this was a valid approach to model the process. The model equations for the velocity profile only were solved in two ways: employing the commercial CFD program FIDAP and a finite-difference program developed for this model. Both methods produced valid results for this particular problem.

The finite-difference method with improvements can be used for complex simulations, but developing such a comprehensive numerical code is time consuming. The FIDAP code, validated for this particular problem is a better choice to further analyze the issues. The comparison study clearly indicated the applicability of FIDAP for this particular problem.

Acknowledgement: The authors acknowledge Mr. Peter Gerhardinger of Engineered Glass Products, LLC for initiating this study and providing partial financial support. Support was also provided by the Department of Chemical & Environmental Engineering of the University of Toledo.

References

Abdallah, S. (1987): Numerical solutions of the incompressible Navier-Stokes equations in primitive variables using a non-staggered grid *J of Comp. Phys*., vol. 70, pp. 193-202

Chorin, A.J. (1997): A numerical method for solving incompressible viscous flow problems *J of Comp. Phys*., vol. 135, pp: 118-125.

Callies, G.A.; Albach, E.R.; Conour, J.F.; Herrington, R.A. (1987). US Patent 4,661,381.

Curtis, B.J.; Dismukes, J.P. (1972): Effects of natural and forced convection in vapor phase growth systems *J Crystal growth*, vol. 17, pp. 128-140.

Dean, J.A. (1992): *Lange's Handbook of Chemistry*. McGraw-Hill.

FIDAP (1998): *FIDAP 8.0 Theoretical Manual.* Fluent Incorporated.

Gordon, R.G. (1997): Chemical vapor deposition of coatings on glass *J. of Non-Cystalline Solids*, vol. 281, pp. 81-91.

Lawrence, J.G.; Dismukes, J.P.; Nadarajah, A. (2007): Modeling a Discontinuous CVD Coating Process: II. Detailed Simulation Results *FDMP: Fluid Dynamics & Materials Processing*, vol.3, No.3, pp.255-264.

McCurdy, R.J. (1999): Successful implementation methods of atmospheric CVD on a glass manufacturing line *Thin Solid Films*, vol. 351, pp. 66-72.

Meyyappan, M. (1995): *Computational Modeling in Semiconductor Processing*, Artech House.

Perry, R.H.; Green, D. (1984): *Perry's Chemical Engineers Handbook.* McGraw-Hill.

Pozrikidis, C. (2001): *Fluid Dynamics Theory, Computation and Numerical Simulation*. Kluwer Academic.

Slattery, J.C. (1999): *Advanced Transport Phenomena*. Cambridge University Press.

Welty, J.R.; Wicks, C.E.; Wilson, R.E. (1984): *Fundamentals of Momentum, Heat and Mass Transfer*. John Wiley & Sons.

Zhu, M. (2000): US Patent 6,103,015.